MoLoc: Unsupervised Fingerprint Roaming for Device-free Indoor Localization in a Mobile Ship Environment

Mozi Chen, *Student Member, IEEE,* Kezhong Liu, Jie Ma, Xuming Zeng, Zheng Dong, *Member, IEEE,* Guangmo Tong, and Cong Liu *Member, IEEE,*

***Abstract*—Device-free indoor localization may play a critical role in improving passengers' safety in large vessels, particularly for scenarios without equipped radios. However, due to dynamic internal and external influences from the sailing ship such as changing sailing speed, existing localization systems suffer huge accuracy degradation in a mobile ship environment. The challenges are mainly due to rich and arbitrary ship motions and the resulting complicated impacts on the indoor wireless channels. To address the challenges, in this paper, we first propose a ship motion descriptor to extract discriminative latent representation from complex ship motions by leveraging deep-learning techniques. Based on this representation, we then design a novel *fingerprint roaming* model, i.e., MoLoc, to automatically learn the predictive fingerprint variation pattern and transfer the online fingerprint measurement to adapt to dynamic ship motions in real-time. Furthermore, an unsupervised learning strategy is proposed to train the fingerprint roaming model using unlabelled onboard collected data which does not incur any labor costs. We have implemented and extensively evaluated MoLoc on real-world cruise ships, where experimental results demonstrate that MoLoc improves localization accuracy from 63.2% to 92.8% compared to the state-of-the-art localization methods including Pilot, LiFS, SpotFi, and AutoFi, while achieving a mean error of 0.68m.**

***Index Terms*—Passive human localization, Mobile ship environment, Unsupervised learning**

I. Introduction

Amongst all the operational considerations of the modern maritime industry, passengers' safety is the most critical issue ever since the RMS Titanic tragedy in 1912. Real cases that have happened recently (e.g., the 2014 Sewol Ferry Disaster [1]) continue to reveal the tragic consequences of chaotic evacuation and rescue on large vessels, which lacks appropriate coordination of passengers and crew. In the event of such catastrophes, accurate passive **device-free** human localization systems, which localize the individuals not equipped with a radio device, have been proved to be critical in the associated rescue/evacuation operations and improving passengers safety [2].

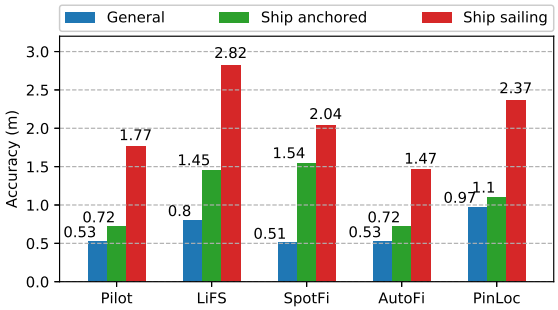

Fig. 1. State-of-the-art localization system evaluation on an actual ship.

Unfortunately, while there have been significant advances in passive human localization, an accurate device-free localization system for such a mobile ship environment is still absent. The recent progress of passive localization mainly focuses on WiFi-based techniques [3] [4] [5] [6] [7] for its ubiquitous infrastructure and being less privacy intrusive compared to video monitoring. However, the state-of-the-art methods, either based on fine-grained channel state information (CSI) or coarse-grained received signal strength (RSS), are facing significant shortcomings in a mobile ship environment due to their vulnerability coping with environmental changes [8] [9]. Contrast to general static scenarios (e.g. office buildings), the mobile ship indoor environment may exhibit immediate, dynamic and unpredictable changes during voyages [10] [11]. The ship is subject to inevitable dynamic (elastic) hull deformations caused by the internal and external stress from the load, waves, and engines during its voyages [12] [13]. Through our extensive experiments conducted on a real-world cruise ship, five state-of-the-art localization systems, i.e., Pilot [5], LiFS [6], SpotFi [14], AutoFi [8] and PinLoc [15], are facing a huge accuracy degradation when ship sets sailing as shown in Fig. 1 (see Sec. VI for experimental details). Existing localization solutions, either based on angle-of-arrive (AoA), fingerprint or attenuation model, all suffer from ship sailing-induced impacts.

M. Chen is with the School of Navigation, Wuhan University of Techology, Wuhan 430063, China (e-mail: chenmz@whut.edu.cn).

K. Liu and J. Ma are with the School of Navigation, Wuhan University of Technology, Wuhan 430063, China, National Engineering Research Center for Water Transport Safety, Wuhan 430063, China and Hubei Key Laboratory of Inland Shipping Technology, Wuhan 430063, China (e-mail: kzliu@whut.edu.cn; majie@whut.edu.cn.

X. Zeng is with the School of Navigation, Wuhan University of Techology, Wuhan 430063, China (e-mail: zengxuming@whut.edu.cn).

Z. Dong is with the Department of Computer Science, Wayne State University, Detroit, MI 48202, USA (e-mail: dong@wayne.edu)

G. Tong is with the Department of Computer and Information Sciences, University of Delaware, Newark, DE 19716, USA (e-mail: amotong@udel.edu)

C. Liu is with the Department of Computer Science, The University of Texas at Dallas, Dallas, TX 75080, USA (e-mail: cong@utdallas.edu)

* Corresponding author: Kezhong Liu (kzliu@whut.edu.cn).

Challenges. To achieve high-precision WiFi-based passive human localization in a sailing ship, we observe from extensive real-world experiments that the mobility of the ship represents one of the main obstacles and brings three hard challenges: (1) Due to the richness and dynamics of outdoor sailing factors which may introduce environmental changes (such as sailing speed, acceleration motion, turning motion, weather condition and altitude), analyzing and modeling the impact of each factor is inefficient and impractical. (2) To adapt the existing localization methods in a dynamic mobile ship environment, it requires exploring the model parameters at all possible sailing conditions, which is (if ever possible) labor-intensive and time-consuming and may cause unaffordable system deployment cost. (3) For capturing the slight changes of hull deformation in such environment, the resolution of CSI measurement using commercial WiFi infrastructures is limited by its bandwidth, which would bring uncertainty of channel measurement for the data analysis. These three technical challenges should be carefully addressed to achieve the high resolution and stable passive localization in a mobile environment.

Contributions. To address these challenges, in this paper, we propose MoLoc, an online deep learning framework which develops a practical solution for passive human localization in the mobile ship environment. MoLoc is able to learn the motion-related CSI variation pattern using unlabelled CSI data and automatically transfer the online CSI fingerprint to adapt to dynamic mobile ship environment. To achieve this goal, the design of MoLoc contains the following key components. First, facing the multiple external environment factors, we propose a motion descriptor using convolutional autoencoder technique to find latent representations of complex ship sailing conditions and avoid individually modeling each factor's impact. Second, to overcome the CSI resolution limitation, we propose CSI embedding layer to project CSI measurements into a higher-dimensional sparse space to process the slight changes of signal propagation using deep learning technique. Third, a Long Short-Term Memory (LSTM) based *fingerprint roaming* model is proposed to learn the predictive fingerprint variation introduced by ship motions and intelligently transfer the online fingerprints to adapt to the mobile environment. Furthermore, for the data collection cost consideration, we propose an unsupervised learning strategy to utilize unlabelled CSI measurements and ship onboard sensors to automatically train the roaming model, which can significantly reduce the overall system deployment cost.

We have implemented a prototype MoLoc system using COTS Intel 5300 cards with existing onboard WiFi infrastructures and deployed onboard an actual passenger ship. In the current MoLoc, the sensors data are collected using smartphones deployed in the ship, and we use a desktop with Intel CPU and Nvidia GPU for neural network training. We conduct experiments in indoor space with dynamic/static users on a real-world cruise ship. Based on our evaluations, compared to state-of-the-art localization methods including Pilot, LiFS, SpotFi, and AutoFi, MoLoc improves localization accuracy from 63.2% to 92.85% and achieves a mean error of 0.68m in dynamic ship sailing conditions.

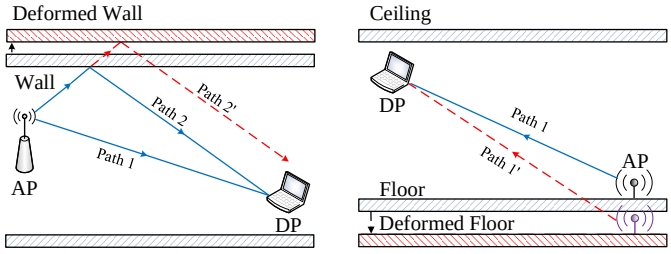

(a) Case 1. (b) Case 2.

Fig. 2. Illustrate how ship deformation affect wireless signals.

II. Practical Challenges

MoLoc addresses significant drawbacks of current localization techniques with commercial wireless infrastructure applied in a mobile ship environment. Aiming to overcome the mobile environmental effects, in the following, we demonstrate three practical challenges for building a ubiquitous WiFi-based indoor localization system in a ship environment.

Arbitrary Ship Motions. WiFi-based indoor localization techniques mostly rely on exploring the slight difference of signal propagation, reflection and absorption introduced by the existence of the people. Thus, these methods are vulnerable to the subtle environmental changes, which may confuse the CSI measurements caused by the localized targets. However, based on our observation, the ship deformation caused by ship motions can significantly influence the indoor wireless signal propagation as shown in Fig. 2. When voyaging, the ship's hull is subject to inevitable deformations, including static angular deformation and dynamic angular deformation, caused by the external stress of loads, waves, and external temperature changes [12]. The ship static angular deformations can amount to 1° due to the redistribution of freight and fuel. The non-uniform heating of different ship parts under the sun also may lead to up to 1° change. As for the dynamic angular deformations, they are caused by hull motion, wave impact, helm steering, and can be as high as 1°–1.5° [**?**] [13].

Owing to these deformations of the sailing ship, the angular position of peripheral equipment (radar antennas, WiFi antennas) may differ significantly from the original devices setup parameters. Therefore, ship environmental effects from hull deformation related to its various sailing motions including different speed, accelerations, rotation and weather during its voyage. Meanwhile, the ship motions during the different sailing conditions are remarkably arbitrary due to the ship driving operations are complex and mainly based on the crew's experience. For instance, when a sailing ship detects an approaching ship on its way, avoiding actions would be a complex and experience-depended process. Before taking any actions, the encounter situation, safety distance, visibility, counterpart's intentions, weather conditions are considered by the crew. Operators then determine the ship avoidance actions, including turning amplitude, turning time and avoidance ranges, mostly according to their experience. Therefore, the sailing condition and ship motions are diverse and unpredictable during its voyages. It is extremely hard to find and quantify their motions to cover all rich sailing states.

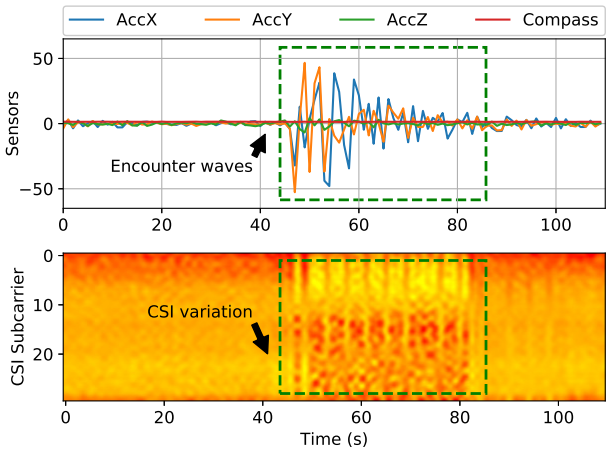

Fig. 3. CSI profile collected during ship voyages.

Diverse Mobility Impacts. Fig. 3 shows an example of the CSI sequences collected in a ship room during its voyage. As can be seen, when the ship sails smoothly without any acceleration or turning, the CSI sequence holds quite stable. However, after the ship encounter waves, which shook the ship hull and lead to the accelerations changes of X-axis and Y-axis (under stress), CSI measurements significantly varies accordingly. The variation shows a close correlation with ship sailing conditions and introduces the unacceptable huge interference to the current wireless indoor localization systems. In this case, due to the wide variety of ship motions, modeling all patterns of mobile ship environmental impact on indoor CSI behaviors in a human-depended way is unrealistic. Exploring all possible sailing conditions is (if ever possible) labor-intensive and time-consuming, which cause unaffordable system deployment cost in any practical settings.

CSI Resolution Limitation. CSI is fine-grained physical layer information that describes wireless channel at frequency domain which can be denoted by

$$H(f_i) = |H(f_i)|e^{jsin(\angle H(f_i))} \quad (1)$$

where f_i is the central frequency of subcarriers ($i = 1, ..., M$), $|H(f_i)|$ denotes its amplitude and $\angle H(f_i)$ denotes the phase. To explore the CSI variation reason in the mobile ship, we could physically analysis the multipath changes introduced by hull deformation as shown in Fig. 2. It can be seen that slight hull deformation would change the locations of the transmitter and receiver, which alter the multipaths, even the line-of-sight path in the environment. To quantify these changes, theoretically, CSI can be converted through IFFT (Inverse Fast Fourier Transform) to time-domain power delay profile, which can characterize the multipath channel. However, due to the bandwidth limitation on commodity WiFi NICs, the time resolution of the derived power delay is incapable to distinguish such subtle multipath changes. For the widely used 20MHz bandwidth, the resolution is $1/20\text{MHz} = 50\text{ns}$, which leads to 15m resolution for detecting the path lengths [16]. For a finer-grained hull deformation, the needed bandwidth may not impossible for current commodity WiFi NICs.

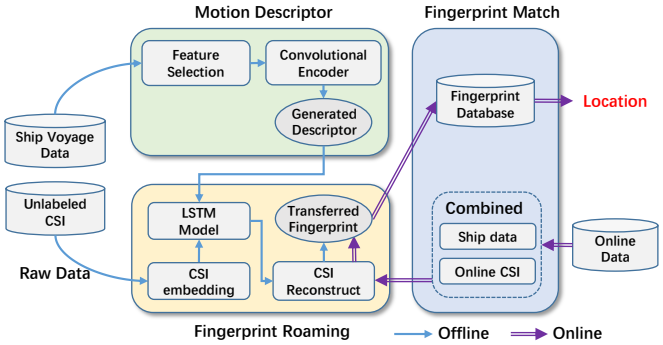

Fig. 4. MoLoc Overview.

III. System Overview

The focus of our work is on enabling WiFi-based device-free indoor localization (1) to work efficiently in the mobile ship environment by considering a set of ship motion impact factors, and (2) to achieve the fingerprint transfer without gaining any human effort by utilizing unlabeled WiFi collected data. As shown in Fig. 4, MoLoc consists of three components: mobility descriptor, *fingerprint roaming* and fingerprint localization technique.

- **Motion Descriptor**: Facing the richness, dynamics, and unpredictability of the ship motion, we propose a motion descriptor for extracting discriminative latent representation of diverse ship motions from multiple shipborne sensors data without prior knowledge of the experts.
- **Fingerprint Roaming**: To avoid labor-intensive collecting and annotating CSI variation data, a *fingerprint roaming* model, which is a well-designed neural network with an unsupervised learning strategy, is proposed to learn from the massive unlabelled CSI data combined with ship sensors and to transfer the impacted fingerprints to adapt to the pre-trained model. In addition, a CSI embedding layer is designed to overcome the resolution issue.
- **Localization Model**: Based on our *fingerprint roaming* model, we propose an online fingerprint inference method and build a device-free human indoor localization model by considering the multiple factors of ship motion states and the real-time CSI measurements.

The details of CSI measurement and fingerprint database follow the regular practice in academia (e.g., [5]). Thus, we skip these and focus on the new designs in MoLoc: the motion descriptor and the *fingerprint roaming* model.

IV. Mobility Descriptor

As mentioned above, the system should be capable of considering arbitrary ship motion which related to multiple series of sensors data. To achieve this goal, we are looking for a ship sailing state extraction method to automatically classify ship sensor information into various ship motions and represent them by low dimensional vectors called motion descriptors. Inspired by the vector space basis from linear algebra, we propose the concept of ship motion basis to

capture the discriminative sensors features and an unsupervised autoencoder machine to obtain these motion basis. We introduce each step in detail as follows.

A. Data Collection

The first step is to collect the ship motions-related sensors data from real-world ships. In this work, we deployed several sensors (e.g., accelerometer, gyroscope, magnetometer and compass) and WiFi infrastructures in an inland cruise ship namely "Yangze 7" to simultaneously collect the on-line WiFi channel data and ship motion information. We considered a set of motion factors of a mobile ship environment: 1) day time, 2) location coordinates, 3) speed, 4) 3-axis acceleration, 5) compass, 6) weather (barometric pressure and temperature) and 7) engine state (measured by engine sound). The CSI is utilized to measure the channel properties of the communication link in the ship indoor environment. We record these data in "Yangze 7" during its five voyages (25 days in total) and pack them into a matrix structure for next learning procedure.

Here, the total n packets of m subcarriers CSIs collected in an empty room with the period of 100 ms are combined into a CSI matrix $\mathbf{H} = [H_1, H_2, \ldots, H_n]$. The corresponding related ship sensors information: brightness $B = [b_1, b_2, ..., b_n]^T$, ship speed $V = [v_1, v_2, ..., v_n]^T$, 3-axis acceleration $A = [A_x, A_y, A_z]^T$, ship location coordinates $L = [l_1, l_2, ..., l_n]^T$, magnetism measured by magnetometer $M = [m_1, m_2, ..., m_n]^T$, temperature of indoor environment $T = [t_1, t_2, ..., t_n]^T$ and air pressure $P = [p_1, p_2, ..., p_n]^T$ are represent to a matrix $\mathbf{X}$:

$$\mathbf{X} = [B, V, A_x, A_y, A_z, L, H, M, T, P] \tag{2}$$

Among them, the sparser sensors data with lower sampling rates are preprocessed with interpolation to align with CSI timestamps. Meanwhile, the outliers caused by sensor internal errors are also removed with an outlier filter.

B. Factors Selection

Next, before finding the ship motion basis from the packed diverse ship sensors data, we measure the correlation between motion factors and CSI variation to select the primary factors and reduce trivial randomness from the world. Here, we adopt principal components analysis (PCA) to find the principal components of CSI variation and Pearson correlation coefficient (PCC) to obtain the main influence factors.

Since CSI is composed of power attenuation from m subcarriers, PCA can be utilized to find the lower-dimensional projection that best represents the variation of CSI data set. We first standardize the CSI matrix $\mathbf{H}$ as $\hat{\mathbf{H}}$ to ensure that all the subcarriers information are treated on the same scale. Then the PCA transformation basis A can be obtained by selecting the maximum-variance directions as follows:

$$A_{opt} = \arg\max_{A} |A^T \Sigma A| \tag{3}$$

where Σ is the covariance matrix of all vectors of $\hat{\mathbf{H}}$. The solution $A = [e_1, e_2, ..., e_m]$ is in fact a subset of eigenvectors

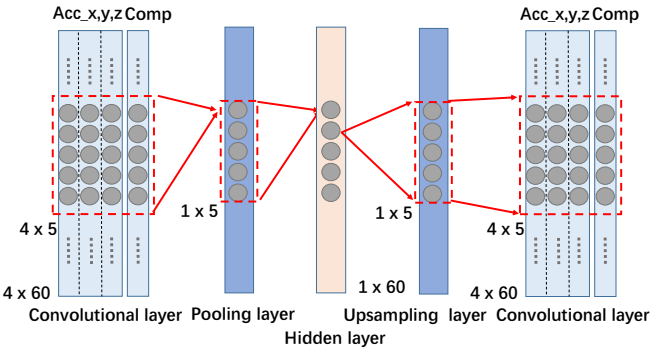

Fig. 5. Convolutional Autoencoder Machine.

of Σ, where e_i is the i-th eigenvector obtained from the eigen-decomposition of the matrix Σ. The first two principal components with the highest eigenvalues are selected to combine as a transformation matrix $A_p = [e_1, e_2]$ to calculate the 2-D projection Y_p by

$$Y_p = A_p^T \hat{\mathbf{H}} \tag{4}$$

where Y_p is a $n \times 2$ matrix that contains most of information of $\hat{\mathbf{H}}$. Based on the projection Y_p, PCC is utilized to measure the correlation between each sensor factor with the CSI variation Y_p. After normalizing and outlier filtering the sensors data to $\hat{X}$, Pearson correlation coefficients ρ can be obtained by:

$$\rho_{X_i, Y_i} = \frac{\mathbb{E}(\hat{X}_i - \bar{X}_i)(Y_i - \bar{Y}_i)}{\sigma_{X_i} \sigma_{Y_i}} \tag{5}$$

where Y_i denotes the i-th principle projection of CSI and $X_i \in \{B, V, A_x, A_y, A_z, L, H, M, T, P\}$ is the ship sensors data. $\bar{X}$ and $\bar{Y}$ represent the mean value of each sensor vector respectively. The value of ρ is between $[-1, 1]$, which denotes a positive or negative correlation. The sensors factors with the highest correlation coefficient can then be selected for the next motion basis learning.

C. Motion Learning

To learn the latent representation of ship motions, in this part, we utilize Convolutional Auto-Encoder (CAE) [17] to find the ship motion basis from the real-world sensors data through unsupervised learning. CAE is a neural network for "encoder" and "decoder" data with convolutional layers to discover localized features that repeat themselves all over the input. In the proposed method, we use multi-layer architecture to extract features as illustrated in Fig. 5. The network architecture consists of three basic building blocks, including a convolutional layer, a max-pooling layer, and a dense-connected layer, to be stacked as needed.

The selected features X_i are formed as input matrix I with the size of $D_T \times D_K$, where D_T is the length of time window, also refers to the number of samples, and D_K is the number of sensor axis (e.g. 4 axes is shown in Fig. 5). In our case, $D_T = 60$ to represent 6 seconds for a reasonable period of real-world ship motion. In the convolution layer, 2D kernels are used as the filters, followed by a rectified linear unit (ReLU) to introduce nonlinearity. For the input matrix I, M convolution

kernels W_c^m, whose size are $n_W \times n_W$, are used to map the same size units from input layer to M channels in max-pooling layer:

$$\begin{aligned} h_c^m &= \sigma_c(I * W_c^m + b_c) \\ \sigma_c(x) &= max(0, x) \end{aligned} \tag{6}$$

where the b_c is bias, σ_c is a ReLU function for activation, and $*$ denotes the 2D convolution. For multi-factor nature of ship motion, a max-pooling layer [18] is used to improve filter selectivity, as the activation of each neuron in the latent representation is determined by the matching features and input field over the region of interest. Max-pooling layer down-samples $h_c = [h_c^1, h_c^2, \ldots, h_c^M]$ to h_m by a constant kernel with the size of $1 \times n_p$, which taking the maximum value over none overlapping sub-regions, and shrink the length into $(D_T - n_W)/n_p$. Before the last hidden layer, a dense-connected layer with weights W_d follows to linear combine each row of down-sampled h_m and through a sigmoid function into n_h length of hidden layer states h_v:

$$\begin{aligned} h_v &= \sigma_d(h_m * W_d + b_d) \\ \sigma_d(x) &= \frac{1}{1 + e^{-x}} \end{aligned} \tag{7}$$

Based on the principles of auto-encoder models, followed by "encode" phase, where the multiple sensors I have transformed into lower description h_v, the "decode" phase is then used to reconstruct the decoded h_v back to I by a reverse mapping. The reconstruction procedure includes reverse layers, up-sampling layer as shown in Fig. 5. We can obtain the reconstruction by $y_d = \sum_k h_v * \tilde{W}_d + a_d$ and $y = \sum_k y_c * \tilde{W}_c + a_c$, where $\tilde{W}_d$ and $\tilde{W}_c$ are the reverse of W_d and W_c. For CAE, the training goal is to learn the convolutional kernels W_c and dense layer weight W_d that can extract the latent representation information of the data I. With little information lost of the lower-dimensional description, h_v can be reconstructed to the original I. In other words, to train such a model, the learning process is described simply as minimizing a loss function of the mean squared error (MSE) of reconstructed y and input I:

$$E(W_c, W_d) = \frac{1}{2n} \sum_{i=1}^{n} (I_i - y_i)^2 \tag{8}$$

where n is total samples of CAE training. Therefore, an unsupervised training can be achieved by standard backpropagation method [19], which we skip for the length consideration. Just as for standard networks to compute the gradient of the error function with respect to the parameters. Based on the trained encoder network, the motion basis can be obtained as the "encoder" model of CAE with the parameters of convolution kernels W_c and dense layer weights W_d.

After the motion basis is learned, the descriptor v of ship motion can be obtained from an input ship sensors data matrix I and denoted as

$$v = \text{ CAE }_{W_c, W_d}(I) \tag{9}$$

Afterwards, the desired motion descriptor v can be used for next *fingerprint roaming* model.

V. Fingerprints Roaming & Localization

Based on the proposed motion descriptor, we can then explore the pattern between CSI profile variation and diverse ship motions. However, to construct a CSI transfer model for pre-built fingerprint database using supervised learning, it is too expensive to collect fingerprints variation data from all locations during all ship motions period. To overcome this challenge, in this section, we propose an LSTM-based CSI transfer learning model with an unsupervised learning strategy, namely *fingerprint roaming*, to automatically learn the transferred fingerprint map for accommodating all motions of a sailing ship. At last, a fingerprint-based localization method is introduced.

A. CSI Embedding

As described in Sec. II, the hull deformation introduced by ship motions includes two kinds of effects may apply on multipaths: some multipaths are enhanced or weaken and some are delayed or forward. We take Fig. 2(a) as an example, as a wall imperceptibly deformed when the ship sets sailing, $Path2$ was replaced by new $Path2'$ as the shape of the reflection surface deformed. Since the new signal of $Path2'$ propagates through a longer distance, the path power would be weakened and delayed compared to the previous situation. This would bring a constant magnitude scaling and a time delay shift on the original power delay profile. However, for the widely used 20MHz bandwidth in 802.11n, the time resolution of the derived power delay profile from CSI is 50ns. The influenced signal power would be confused with the power of its following signals as shown in Fig. 6.

To address this problem, we propose a CSI embedding method which can decompose and reconstruct WiFi path signal in high time resolution using deep learning technique. The embedding layer and reconstruction layer are shown in Fig. 7. In this layer, we first convert the CSI profile from frequency-domain to time-domain by IFFT. Meanwhile, CSI phase error, e.g., sampling frequency offset and packet boundary detection error, are removed according to [16]. Then the m dimension estimated power delay profile are embedded to a $K_e \times m$ dimensional sparse space, where K_e is the number of neurons connected to one input channel. Similarly, the reconstruction layer recomposes the power delay profile from the same space and convert it back to CSI using FFT. In this part, we denote the weights of CSI embedding layer and reconstruction layer as W_e and W_r.

B. LSTM-based Transfer Model

Based on CSI embedding which can decompose and reconstruct CSI signal, we now propose a deep learning framework which can capture the signal variation pattern of different ship motion descriptors and reconstruct the CSI profiles to adapt to target ship motion. Inspired by recent advances in deep learning, it is possible to construct a powerful "end-to-end" CSI transfer model by maximizing the correct CSI reconstruction at each ship motion states. Thus, we propose to directly maximize the probability of the accurate CSI

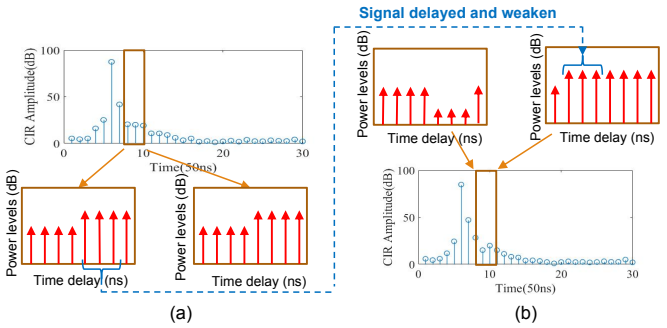

Fig. 6. Effect of signal path changing on CSI measurement. (a) before hull deformation, (b) after hull deformation

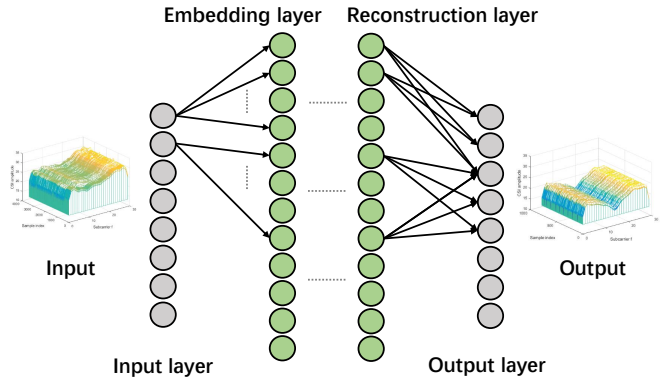

Fig. 7. CSI Embedding Layer.

reconstruction H_g given the source CSI profile H_s by using the following formulation:

$$\theta = \arg\max_{\theta} \sum_{(H_g, H_s, \delta_{s,g})} \log p(H_g|\delta_{s,g}, H_s; \theta) \tag{10}$$

where θ are the parameters of our model, $\delta = (v_s, v_g)$ denotes the ship motion change and contains two variables: v_s denotes source ship motion descriptor and v_g is target descriptor. Since H_g represents a CSI profile series during the time window of v_g, its length equals D_T according to last section. We can model the joint probability of the CSI sequence by chain rule:

$$\log p(H_g|\delta_{s,g}, H_s) = \sum_{i=0}^{D_T} \log p(H_g^{(i)}|\delta_{s,g}, H_g^{(0)}, \cdots, H_g^{(i-1)}) \tag{11}$$

To model the sequence $p(H_g^{(i)}|\delta_{s,g}, H_g^{(0)}, \cdots, H_g^{(i-1)})$, it is common to use recurrent neural network (RNN). Meanwhile, due to there are two elements in the critical parameter $\delta_{s,g}$: source state v_s and target state v_g, we adopt LSTM cell [20] to model this sequence for the similarity that there are two inner states in an LSTM cell.

A LSTM cell contains a hidden state h, cell state c, and three gates: forget gate f, input gate i, and output gate o. The c and h would be initiated with v_s and v_g. In every step, input $H_g^{(t)}$ is stacked with previous hidden state h_{t-1} and multiply by LSTM weights W_L to decide the values of all gates and variable g. The three gates are used to determine current inner states h_t and c_t. Among them, f decides whether to forget the previous state c_{t-1}, i decides whether to read new input $H_g^{(t+1)}$ and determine the current cell state c_t with g. At the end, the current state h_t is calculated by o and c_t. The definition of the LSTM cell update is as follows:

$$\begin{pmatrix} i \\ f \\ o \\ g \end{pmatrix} = \begin{pmatrix} \sigma_L \\ \sigma_L \\ \sigma_L \\ \tanh \end{pmatrix} W_L \begin{pmatrix} h_{t-1} \\ H_g^{(t)} \end{pmatrix} \tag{12}$$

$$c_t = f \odot c_{t-1} + i \odot g \tag{13}$$

$$h_t = o \odot \tanh(c_t) \tag{14}$$

Here, $\odot$, σ_L and $\tanh$ represent the element-wise multiplication, logistic sigmoid activation and hyperbolic tangent function respectively. W_L is weights of LSTM cell which is for CSI sequence transfer. Such two inner states RNN cell makes it possible in our system to model the mobile environment phases changing and learn such variation patterns of CSI profile at each environment states transition automatically.

C. Fingerprints Roaming

In this part, we propose an unsupervised learning strategy to train the *fingerprint roaming* model utilizing unlabelled CSI measurements in the ship with their corresponding ship sensors information. In MoLoc, a **CSI fingerprint** F_l is defined as a combination of a location label and a set of CSI profile when a person is at location l:

$$F_l = \{[H_1, H_2, \cdots, H_N]; l\} \tag{15}$$

Here, a total of N packets of CSI profile are recorded in a fingerprint. For the human localization, we select L locations in the interested area and record CSI fingerprint at each location to build a fingerprint map $F = (F_0, \cdots, F_L)$. In the measurement, if we keep monitoring the variation of F_l during the ship voyage and record the corresponding ship sensors data X_k. The records can be denoted by a **fingerprint profile** G_l in mobile ship environment:

$$G_l = \{(F_l^0, X_0), (F_l^1, X_1), \cdots, (F_l^K, X_K)\} \tag{16}$$

where F_l^k is fingerprint when the ship is at motion state of X_k and K denotes the total number of fingerprint profiles.

Unlabelled Data. In the system running phase, assuming that the runtime is long enough while passengers stay on board, we can obtain long-term unlabelled CSI profiles (refers to the CSI measurements without knowing the human location) and the corresponding sensors data, which can cover all interesting locations and the ship motions either. As an example, a passenger would roam in the area for the whole voyage, so the system can collect the unlabelled CSI profiles which contain all interesting locations $\{F_0, F_1, \cdots, F_L\}$. For the voyages are long enough, the collected CSI profile would cover all ship motions $\{X_0, X_1, \cdots, X_K\}$ either. Meanwhile, CSI variation caused by human moving can be eliminated by human moving detector [21]. Combined all this information, complete fingerprint profiles $\{G_0, G_1, \cdots, G_{-L}\}$ without human location can be obtained for our model training.

Unsupervised Learning. MoLoc is trained to predict the CSI fingerprint changes when ship motion transition from

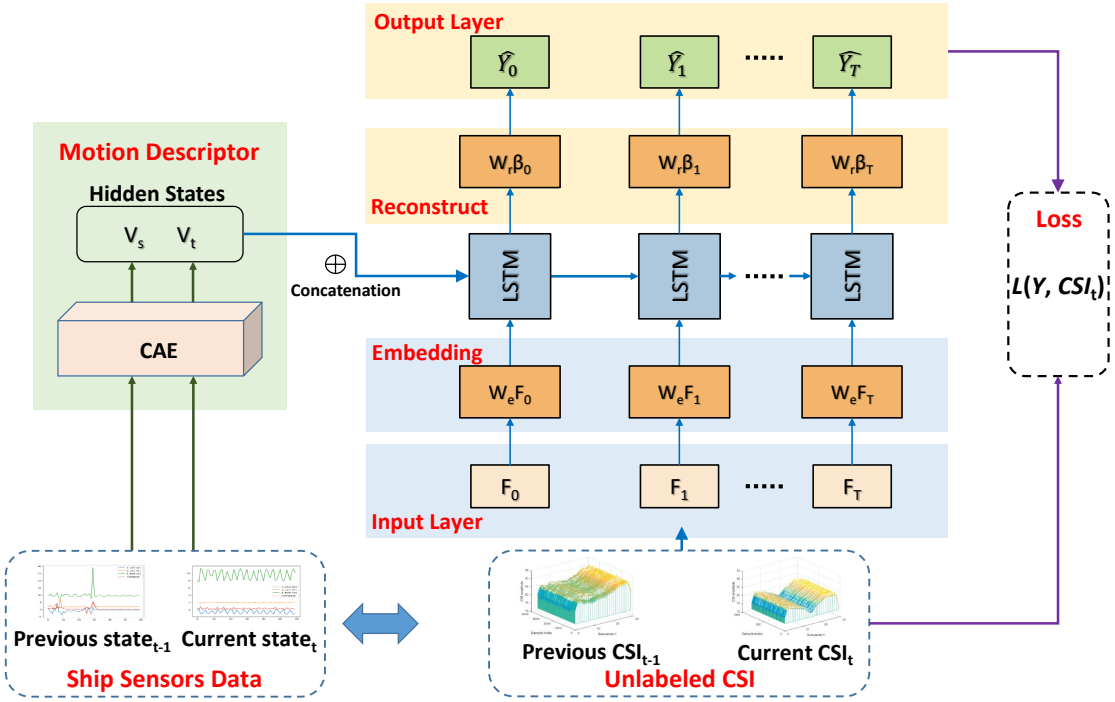

Fig. 8. Unsupervised training strategy of *fingerprint roaming* model.

source motion to target motion. The training strategy is shown in Fig. 8. To train such model, firstly, the two ship motion data X_{k-1} and X_k are fed to CAE model to obtain two ship motion descriptors v_s and v_g, which are directly sent to LSTM cell as the two initial inner states. Then, the fingerprint F_l^{k-1}, which correspond to X_{k-1}, are export to CSI embedding layer and obtain α_{k-1} as the input sequence of LSTM. Based on cell gates, LSTM keeps emitting β_k which is in the same space with α_{k-1} can be used to estimate the predict CSI fingerprint by reconstruction layer. The loss function of the roaming model can be presented as the sum of the negative log-likelihood of the predicted CSI and F_l^k (correspond to X_k) at each step as follows:

$$v_s, v_g = \mathrm{CAE}(X_{k-1}, X_k) \tag{17}$$

$$\alpha_{k-1} = W_E \cdot F_l^{k-1} \tag{18}$$

$$\beta_t = \mathrm{LSTM}_{v_s, v_g}(\alpha_{k-1}) \tag{19}$$

$$Loss = -\sum_i logp_i(F_l^k - W_R \cdot \beta_i)^2 \tag{20}$$

Based on the *fingerprint roaming* model, the online CSI fingerprint affected by ship motion can be used to predict the fingerprint of target ship motion.

D. Online Localization

Aiming to the ship motion of the constructed fingerprint database $\{F_1, F_2, \cdots, F_L; X_M\}$, the predicted CSI fingerprint would be obtained by feeding the target ship state X_M and the real-time CSI to the model. We design the device-free fingerprints matching method based on classifier algorithms, i.e., support vector machines (SVM), which have widely used in fingerprint-based localization [22], to predict locations with fingerprint map. The SVM used here employs a radial basis function (RBF) kernel to project data to a higher-dimensional space, where the RBF kernel on two samples x and x' is defined as

$$K(x, x') = \exp(-\gamma |x - x'|^2) \tag{21}$$

where γ is a kernel size parameters. We utilize open software LIBSVM tools [23] to train and predict the fingerprints. Based on the SVM model, Moloc can finally estimate the locations of new fingerprints obtained by *fingerprint roaming*.

VI. Implementation & Evaluation

We have fully implemented and extensively evaluated MoLoc on two real-world passenger ships. We first describe our testbeds and data collection methodology and then evaluate the performance of MoLoc against four state-of-art human localization techniques.

A. Baseline Methods

We compare MoLoc with four state-of-the-art CSI-based localization techniques Pilot, SpotFi, LiFS, AutoFi in mobile ship environment. Among them, Pilot, which is **Baseline** method, and LiFS are passive localization techniques for a static environment using CSI fingerprint or CSI power fading model to estimate user location. SpotFi is AoA-based localization method using the direct path AoA estimates and RSSI measurements from all the WiFi routers. AutoFi is a state-of-the-art fingerprint-based localization with an online-calibration module to adapt to the dynamic environment such as moving furniture. Comparison of these systems with MoLoc are shown in Table. I. FP and PS stand for fingerprint and phase shift.

TABLE I
A COMPARISON OF STATE-OF-THE-ART WORKS FOR PASSIVE WIFI-BASED LOCALIZATION

Properties	LiFS	SpotFi	Pilot	AutoFi	MoLoc
Technique	Wi-Fi	Wi-Fi	Wi-Fi	Wi-Fi	Wi-Fi
Method	Attenuation	PS/AoA	FP	FP	FP
# (Tx, Rx)	(1, 1)	(2, 2)	(2, 2)	(1, 1)	(1, 2)
Scenario	Static	Static	Dynamic	Dynamic	Dynamic
Range	12m	8m	11m	7m	12m
Accuracy	0.7m	0.6m	1.0m	0.8m	0.5m

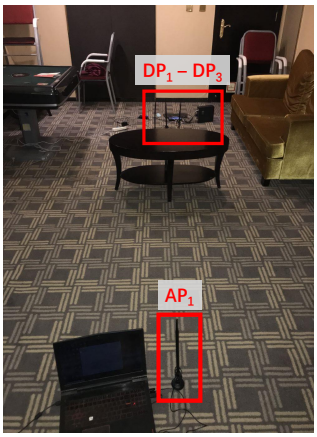

(a) CSI collection in room.

(b) Intel 5300 NIC.

(c) Ship motion detection.

Fig. 9. Experiments scenes in passenger ship 'Yangtze 2'.

B. System Implementation

In the experiments, wireless access points (APs) are TP-LINK routers, operating on 2.4 GHz band with a bandwidth of 20 MHz. Detecting points (DPs) are standard ThinkPad T-series laptops equipped with commercial 802.11n 5300 NICs and the Linux kernel 2.6.34 operating system. Two iPhone 6s smartphones with customized software are used for GPS and ship motion information collection. The system service is set up on a PC with 3.40GHz Intel E3-1231 CPU and 16GB of RAM. MoLoc components are implemented with Python. For the deep neural network, we modify and construct the CAE and LSTM network with TensorFlow and Keras.

We implemented our experimental testbed to collect ship motion and CSI data from four rooms, where the sizes are $6.5m \times 9.4m$ and $9.7m \times 13.2m$, in two different cruise ships, dubbed "Yangtze 2" and "Yangtze 7". In each room, 9 locations are selected for evaluation. The least distance between two nearby locations is 0.4m, which yields a reasonable range for a human to stay. At the experimental rooms, we build CSI infrastructures which include 2 to 3 DPs and 1 AP to cover the area as shown in Fig. 9. To create the localization communication, the DPs constantly ping the APs with a frequency of 10 packets per second (pks). At each location, 300 packets of CSI profiles with the corresponding ship motions data are recorded to establish the passive fingerprint map.

Data Record. During two ship voyages, we employed four volunteers, including both man and woman, as localized

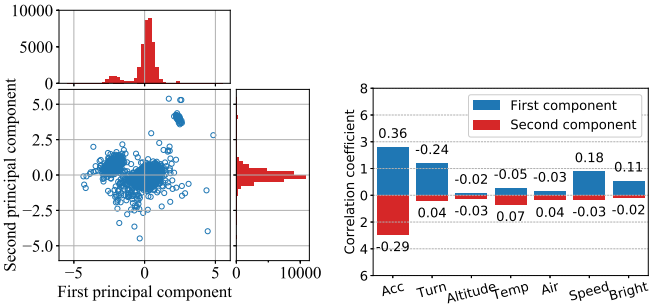

(a) CSI distribution on the first two principal components.

(b) Pearson correlation coefficient of each factor with CSI.

Fig. 10. CSI-Mobility related factors selection.

objects and collect and their unlabelled CSI data and corresponding sensors data in each room. The volunteers are asked to repeatedly stay at each location during the voyages with both sitting and standing activities, as we collected fingerprint map previously. During a five-day voyage, the cruise ship stops twice in different ports each day to wait for passengers visiting ashore. Therefore, we can collect 10 rounds of complete ship-to-parking data in one voyage and cover all 9 locations. Totally, we have collected 720 records of unlabelled CSI fingerprints and their corresponding ship motion data (from nine physical locations and four people of twenty round). To objectively evaluate the accuracy of five techniques in mobile ship environment, we collect our **test data set** by randomly choosing 5 different times during a 3-day voyage window to test the CSI-based localization method performance both in day and night, as shown in Table. II.

C. System Performance

The overall performance comparisons in three parts in this section, i.e., motion descriptor, fingerprint roaming, and localization accuracy.

Motion Descriptor. We first evaluate the feature selection method and select our interested sensors data in this part. The results of our case using PCA and PCC are shown in Fig. 10. Among them, Fig. 10(a) illustrates the projections of CSI on the first two principal components: e_1 and e_2. The compressed CSI profiles are scattered and the histograms of each component are also shown. The correlation coefficient of each sensors data with e_1 and e_2 projections are shown in Fig. 10(b). As can be seen that the correlation between acceleration, rotations and speed with CSI are higher than the other factors like air pressure and brightness. Therefore,

TABLE II
TEST DATA SET OF CSI COLLECTION UNDER DIFFERENT TIME.

Set	Test date	Time	Ship speed
1	May 28, 2019 (Day 1)	6:00 PM	0 km/h
2	May 29, 2019 (Day 2)	9:31 AM	21.2 km/h
3	May 29, 2019 (Day 2)	2:05 AM	6.3 km/h
4	May 30, 2018 (Day 3)	12:20 PM	5.6 km/h
5	May 30, 2018 (Day 3)	4:34 PM	9.2 km/h

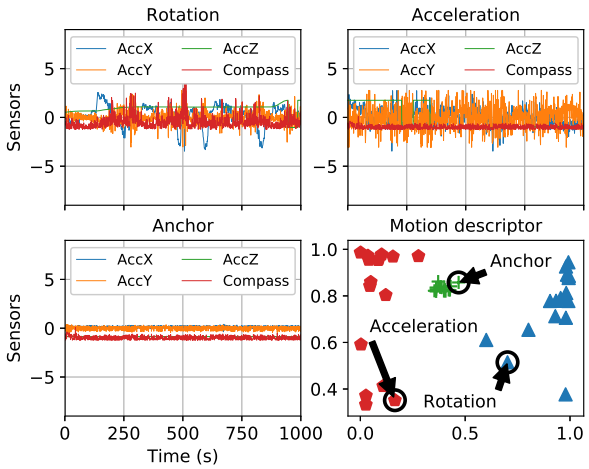

Fig. 11. Raw ship sensors data and motion descriptor analysis.

these three most related sensors information of ship motion are selected for our mobility descriptor.

Then, based on the observation, the motion descriptor is performed to extract the latent representation from ship acceleration, rotation and speed. In our case, the raw data of three ship motion, i.e., anchor, acceleration, and rotation, and the extracted motion descriptor are plotted in Fig. 11. Here we only show acceleration and rotation in each raw data and use 2-D space to represent three motions descriptors. It can be observed that the samples of descriptors can form three clusters, which intuitively demonstrate that the proposed motion descriptor could represent the multiple ship motion into a discriminative space.

Fingerprints Roaming. To further illustrate the effectiveness of our *fingerprint roaming* model, we show how the environmental changes in a mobile ship degenerate the CSI fingerprint-based localization performance. As shown in Fig. 12, the confusion matrices of localization of nine locations are presented to investigate the nature of fingerprint variation under ship motions of Set 2. It is demonstrated in Fig. 12(a) that, when the ship keeps parking at the port, the fingerprint map remains consistent and make the fingerprint-based localization classification achieves a perfect accuracy. However, after the ship sets sailing and introduces the interference of CSI measurements, the fingerprint recognition results tend to confuse locations. As shown in Fig. 12(b), the localization results of baseline method mostly are off-diagonal elements and some of them concentrate around location $L4$.

For AutoFi system, which calibrates the on-line CSI fingerprint by detecting the fingerprint variation of reference location $L0$, that denotes no human in the area, to adapt to the changing environment. The confusion matrix of AutoFi is shown in Fig. 12(c). As can be seen that after the fingerprint map is calibrated, most of the localization results tend to converge to $L8$. The results of the *fingerprint roaming* proposed in MoLoc is shown in Fig. 12(d). We can clearly see that the localization results are now placed along the diagonals of the matrices. This suggests that the *fingerprint roaming* module is able to capture the CSI variation pattern according to ship motion and transfer the CSI fingerprints back to their pre-built state.

TABLE III
KERNEL NUMBER SELECTION.

Kernel number	8	16	32	64	128	256
error	1.15	0.92	0.64	0.43	0.43	0.33
sparsity	0.54	0.54	0.53	0.53	0.53	0.53

Localization Accuracy. The localization performance is then evaluated by five testing data sets and the results are presented in Fig. 13. In the anchored ship environment, the baseline method Pilot achieves high accuracy to over 90% (up to 93.2%) which is consistent with the result in [5]. However, as the ship starts sailing, the maximum accuracy of the Pilot dramatically degrades to 63.2%. The experimental results are similar to the other two tested techniques, SpotFi and LiFS. Both methods achieve good performance when the ship is parked, and the accuracy of the two methods is significantly reduced (up to 3.7 meters) when the ship is sailing.

To evaluate the accuracy of MoLoc, we show the accuracies of our system of five test sets. In this experiment, we downsample the ship sensors data to 10 Hz to fit CSI measurement rate and segment the CSI and its corresponding ship motion every 60 samples, which corresponds to the ship motion of about 6 seconds, to combine them as the input to our *fingerprint roaming* model. Here, our system achieves a fingerprint classification accuracy of 92.85% when the distinction is 0.4m, while the auto-calibration method AutoFi achieves 71.31%. The mean localization error of MoLoc in a sailing ship can achieve 0.68m. This indicates the benefits of our system in localization accuracy in a mobile environment and can capture the deformation pattern of different ship motions.

D. Model Analysis

So far, we have described the performance of indoor localization in a mobile ship scenario. In this part, we discuss the model parameters and efficiency.

Impact of kernel number. It is worth noticing that the kernel number CAE affects the performance of our motion descriptor model. Kernel number in CAE would determine the size of our motion descriptor, and improve the decoding accuracy. However, the over number of kernels will lead to extra cost for storage and model training. Here, we choose two metrics, error and sparsity, to evaluate the CAE model. The error is defined as the mean square error between all the encoded and decoded vectors, and the sparsity is the mean value of all the hidden layer values. According to our experiment, as shown in Table. III, the error reduces as kernel number increase. To optimize the kernel number and model cost, we select 64 kernel as shown in the table that the decrease of error slows down, which we think sufficient for accurate ship motion learning.

Efficiency and Scalability. Since the system is designed with energy efficiency consideration, MoLoc uses only beacons from APs in a single channel. It synchronizes with the beacon-schedules of these APs and periodically wakes

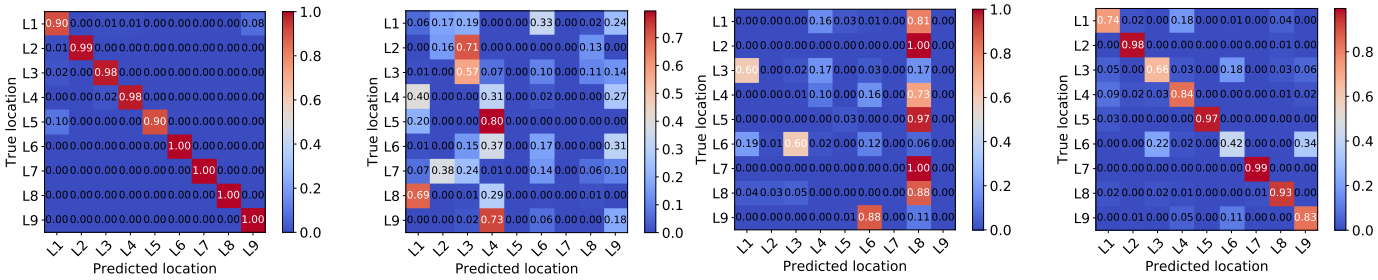

(a) Baseline method (anchored). (b) Baseline method (sailing). (c) AutoFi method (sailing). (d) MoLoc method (sailing).

Fig. 12. Confusion matrices of localization in mobile ship environment.

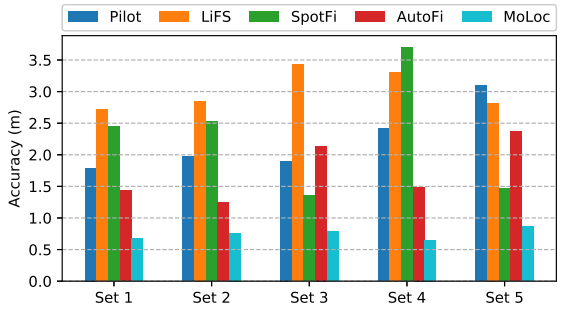

Fig. 13. Comparison of five localization techniques performance in all test set.

up to collect the CSIs. Moreover, because it is more energy efficient to launch a system service than an application, the consumption could be further reduced. To this end, according to our evaluation, keeping running data collecting application at backstage only leads to about 10% additional power consumption, which is affordable for most COTS mobile devices.

VII. Related Works

In this part, we discuss the most relevant works on human passive localization for a mobile ship environment.

Device-free localization. Several RSS-based [24] [25] [26] and CSI-based [28] [**?**] [29] device-free localization and tracking techniques have been proposed as its easy to obtain in commercial off-the-shelf WiFi NICs. The strategies can be divided into two categories: (1) physical model based methods. To localize a target, these works attempt to transform the channel parameters to AoA, Doppler frequency shifts (DFS), or Time-of-Flight (ToF). Among them, MaTrack [4] proposed a novel Dynamic-MUSIC method to extract the object reflection path and estimate the AoA for device-free localization. CARM [7] and Widir [28] exploit DFS to estimate object movement speed to achieve tracking, which however is blindness to static objects. mmTrack [**?**] improves the ToF resolution by leveraging the commodity 60GHz radio and achieves the passively localizes multiple users. Authors in [**?**] concatenate non-adjacent Wi-Fi channels to achieve higher ToF resolution. Widir2.0 [3] build a novel unified model accounting for AoA, ToF, DFS and propose joint parameters estimation using Space Alternating Generalized Expectation-Maximization (SAGE) algorithm. LiFS [6] leverages shadowing effect of targets near line-of-sight of links and an accurate power fading model to estimate the location. (2) machine learning-based method. Based on supervision classifiers (e.g. KNN, SVM, etc.), a signature-location relation model can be established in a site survey. i.e., Nuzzer [25] utilized Wi-Fi RSS as fingerprints to localize a person to one of the fingerprinted locations. Generally speaking, supervised learning strategies can provide better accuracy while require additional human effort to collect labeled data. DeepFi [29] utilized deep neuron network to train all the weights as fingerprints layer-by-layer to reduce complexity.

Dynamic environment. Since WiFi-based localization signatures are sensitive to environmental changes (e.g. people, building layouts et al.), there are a few works consider dynamic environments and efficiency data collection [31] [**?**], i.e., FitLoc [9] designed a transfer scheme using compress sensing to make RSS fingerprint map shared by other different areas. RASID [32] analyzed the RSS behavior and proposed a non-parametric technique for adapting to environmental changes. LEASE [33] employed a number of additional transmitters and receivers to obtain up-to-date RSS values for updating the maps. FitLoc [**?**] design a transfer scheme using compress sensing to make RSS fingerprint map shared by other different areas. The fingerprint data update overhead can be further reduced via crowd-sourced measurements [**?**] [**?**]. AutoFi [8] proposed an auto-calibration approach to collect the CSI of the no-human environment after environment layout changes and predict the fingerprints variation. These methods are not working remarkably in the mobile environment compared with general scenes since the impacts of the mobile environment are complex and fast-changing.

VIII. Conclusion

In this paper, we design and implement one of the first CSI-based passive human localization system for a mobile ship environment. We propose a ship motion descriptor to extract discriminative latent representation from complex ship motions and design a *fingerprint roaming* model with unsupervised learning strategy to automatically transfer the online fingerprint to adapt to dynamic ship motions using unlabelled onboard data. Real-world implementation and evaluation show that MoLoc is able to efficiently improve localization accuracy and significantly reduce the system deployment cost for a mobile ship environment.

ACKNOWLEDGMENT

This work was supported by the National Natural Science Foundation of China (NSFC) under Grant No. 51979216, the Major Project for the Technology Innovation of Hubei Province, China, under Grant No.2017AAA120, the Fundamental Research Funds for the Central Universities under Grant No. WUT-2017-YB-031.

REFERENCES

[1] T. Kim, S. Nazir, and K. I. Overgard, "A stamp-based causal analysis of the korean sewol ferry accident," *Safety Science*, vol. 83, pp. 93–101, 2016.

[2] S. I. Velásquez Correa, M. Castells Sanabra, U. Svedberg *et al.*, "Monalisa 2.0 and the sea traffic management-a concept creating the need for new maritime information standards and software solutions," 2015.

[3] K. Qian, C. Wu, Y. Zhang, G. Zhang, Z. Yang, and Y. Liu, "Widar2 . 0 : Passive Human Tracking with a Single Wi-Fi Link," *ACM International Conference on Mobile Systems, Applications, and Services (MobiSys)*, pp. 350–361, 2018.

[4] X. Li, S. Li, D. Zhang, J. Xiong, Y. Wang, and H. Mei, "Dynamic-music: accurate device-free indoor localization," in *Proceedings of the 2016 ACM International Joint Conference on Pervasive and Ubiquitous Computing (Ubicomp)*. ACM, 2016, pp. 196–207.

[5] J. Xiao, K. Wu, Y. Yi, L. Wang, and L. M. Ni, "Pilot: Passive Device-Free Indoor Localization Using Channel State Information," *2013 IEEE 33rd International Conference on Distributed Computing Systems (ICDCS)*, pp. 236–245, 2013.

[6] J. Wang, H. Jiang, J. Xiong, K. Jamieson, X. Chen, D. Fang, and B. Xie, "LiFS: low human-effort, device-free localization with fine-grained subcarrier information," *Proceedings of the 22nd Annual International Conference on Mobile Computing and Networking (MobiCom)*, 2016.

[7] W. Wang, A. X. Liu, M. Shahzad, K. Ling, and S. Lu, "Understanding and Modeling of WiFi Signal Based Human Activity Recognition," *Proceedings of the 21st Annual International Conference on Mobile Computing and Networking (MobiCom)*, pp. 65–76, 2015.

[8] X. Chen, C. Ma, M. Allegue, and X. Liu, "Taming the inconsistency of Wi-Fi fingerprints for device-free passive indoor localization," *Proceedings of IEEE Conference on Computer Communications (INFOCOM)*, pp. 1–9, 2017.

[9] L. Chang, X. Chen, Y. Wang, D. Fang, J. Wang, T. Xing, and Z. Tang, "Fitloc: Fine-grained and low-cost device-free localization for multiple targets over various areas," *IEEE/ACM Transactions on Networking*, vol. 25, no. 4, pp. 1994–2007, 2017.

[10] M. Chen, K. Liu, J. Ma, and C. Liu, "Spatio-temporal fingerprint localization for shipboard wireless sensor networks," *IEEE Sensors Journal*, vol. 18, no. 24, pp. 10 125–10 133, 2018.

[11] K. Liu, M. Chen, E. Cai, J. Ma, and S. Liu, "Indoor localization strategy based on fault-tolerant area division for shipboard surveillance," *Automation in Construction*, vol. 95, pp. 206–218, 2018.

[12] G. W. Jiang, S. H. Fu, Z. C. Chao, and Q. F. Yu, "Pose-relay videometrics based ship deformation measurement system and sea trials," *Chinese Science Bulletin*, vol. 56, no. 1, pp. 113–118, 2011.

[13] A. V. Mochalov and O. Jo, "Use of the ring laser units for measurement of the moving object deformations," *Second International Conference on Lasers for Measurements and Information Trans. SPIE*, vol. 4680, no. February 2002, pp. 85–92, 2002.

[14] M. Kotaru, K. Joshi, D. Bharadia, and S. Katti, "SpotFi : Decimeter Level Localization Using WiFi," *ACM SIGCOMM computer communication review*, pp. 269–282, 2015.

[15] S. Sen, B. Radunovic, R. R. Choudhury, and T. Minka, "You are facing the Mona Lisa: Spot localization using PHY layer information," *Proceedings of the 10th international conference on Mobile systems, applications, and services*, pp. 183–196, 2012.

[16] Y. Xie, Z. Li, and M. Li, "Precise Power Delay Profiling with Commodity WiFi," *Proceedings of the 21st Annual International Conference on Mobile Computing and Networking (MobiCom)*, pp. 53–64, 2015.

[17] J. Masci, U. Meier, D. Cireşan, and J. Schmidhuber, "Stacked convolutional auto-encoders for hierarchical feature extraction," *International Conference on Artificial Neural Networks*, pp. 52–59, 2011.

[18] D. Scherer, A. Müller, and S. Behnke, "Evaluation of pooling operations in convolutional architectures for object recognition," *Lecture Notes in Computer Science*, vol. 6354 LNCS, no. PART 3, pp. 92–101, 2010.

[19] G.E. Hinton, "Training products of experts by minimizing contrastive divergence," *Neural Computation*, vol. 14, no. 8, pp. 1771–1800, 2002.

[20] O. Vinyals, A. Toshev, S. Bengio, and D. Erhan, "Show and tell: A neural image caption generator," *Proceedings of the IEEE Computer Society Conference on Computer Vision and Pattern Recognition*, vol. 07-12-June, pp. 3156–3164, 2015.

[21] K. Qian, C. Wu, Z. Yang, Y. Liu, and Z. Zhou, "PADS: Passive detection of moving targets with dynamic speed using PHY layer information," *Proceedings of the International Conference on Parallel and Distributed Systems (ICPADS)*, vol. 2015-April, pp. 1–8, 2015.

[22] S.-H. Fang and C.-H. Wang, "A Novel Fused Positioning Feature for Handling Heterogeneous Hardware Problem," *IEEE Transactions on Communications*, vol. 63, no. 7, pp. 2713–2723, 2015.

[23] C.-C. Chang and C.-J. Lin, "Libsvm: A library for support vector machines," *ACM transactions on intelligent systems and technology*, vol. 2, no. 3, p. 27, 2011.

[24] J. Wilson and N. Patwari, "Radio tomographic imaging with wireless networks," *IEEE Transactions on Mobile Computing*, vol. 9, no. 5, pp. 621–632, 2010.

[25] M. Seifeldin, A. Saeed, A. E. Kosba, A. El-Keyi, and M. Youssef, "Nuzzer: A large-scale device-free passive localization system for wireless environments," *IEEE Transactions on Mobile Computing*, vol. 12, no. 7, pp. 1321–1334, 2013.

[26] D. Zhang, Y. Liu, X. Guo, and L. M. Ni, "Rass: A real-time, accurate, and scalable system for tracking transceiver-free objects," *IEEE Transactions on Parallel and Distributed Systems*, vol. 24, no. 5, pp. 996–1008, 2013.

[27] Y. Wang, J. Liu, Y. Chen, M. Gruteser, J. Yang, and H. Liu, "E-eyes: Device-free Location-oriented Activity Identification Using Fine-grained WiFi Signatures," *Proceedings of the 20th annual international conference on Mobile computing and networking (MobiCom)*, pp. 617–628, 2014.

[28] D. Wu, D. Zhang, C. Xu, Y. Wang, and H. Wang, "WiDir: walking direction estimation using wireless signals," *Proceedings of the 2016 ACM International Joint Conference on Pervasive and Ubiquitous Computing (UbiComp)*, pp. 351–362, 2016.

[29] X. Wang, L. Gao, S. Mao, and S. Pandey, "Deepfi: Deep learning for indoor fingerprinting using channel state information," in *2015 IEEE wireless communications and networking conference (WCNC)*. IEEE, 2015, pp. 1666–1671.

[30] Z. Dong, Y. Gu, J. Chen, S. Tang, T. He, and C. Liu, "Enabling predictable wireless data collection in severe energy harvesting environments," in *2016 IEEE Real-Time Systems Symposium (RTSS)*. IEEE, 2016, pp. 157–166.

[31] Z. Dong, C. Liu, L. Fu, P. Cheng, L. He, Y. Gu, W. Gao, C. Yuen, and T. He, "Energy synchronized task assignment in rechargeable sensor networks," in *2016 13th Annual IEEE International Conference on Sensing, Communication, and Networking (SECON)*. IEEE, 2016, pp. 1–9.

[32] A. E. Kosba, A. Saeed, and M. Youssef, "Rasid: A robust wlan device-free passive motion detection system," in *IEEE international conference on pervasive computing and communications (PerCom)*. IEEE, 2012, pp. 180–189.

[33] P. Krishnan, A. Krishnakumar, W.-H. Ju, C. Mallows, and S. Gamt, "A system for LEASE: Location estimation assisted by stationary emitters for indoor RF wireless networks," in *Proceedings of IEEE Conference on Computer Communications (INFOCOM)*, 2004, pp. 1001–1011.

Mozi Chen received the B.S. degree in electric engineering from the Hubei University of Technology, China, in 2013, and the M.S. degree in navigation engineering from the Wuhan University of Technology (WUT), China, in 2016. He is currently a Ph.D. student in WUT. His research work has been focusing on wireless sensing techniques and machine learning algorithms for human localization, emergency navigation and activity recognition in mobile environment, i.e., cruise ships.

Kezhong Liu received the B.S. and M.S. degrees in marine navigation from the Wuhan University of Technology(WUT), Wuhan, China, in 1998 and 2001, respectively. He received the Ph.D. degree in communication and information engineering from the Huazhong University of Science and Techonogy, Wuhan, China, in 2006. He is currently a professor with School of Navigation, WUT. His active research interests include indoor localization technology and data mining for ship navigation.

Jie Ma received the Ph.D. degree in computer science from the Huazhong University of Science and Technology, China, in 2010. He is currently an associate professor in the School of Navigation at the Wuhan University of Technology. His research includes networked sensing systems and data driven intelligent transportation systems, supported by National Natural Science Foundation of China. He has published over 20 journal and conference papers in the related fields.

Xuming Zeng received the Ph.D. degree in the Geodetection and Information Technology from the China University of Geosciences, China, in 2018. He is currently working toward the Postdoctor with the Traffic and Transportation Engineering, School of Navigation, Wuhan University of Technology, China. From 2016 to 2017, he was a joint training Ph.D. student with Electrical and Computer Engineering, Florida State University, Tallahassee, FL, USA. His research interests include routing protocols, and performance analysis, for wireless networks.

Guangmo Tong is an Assistant Professor in the Department of Computer and Information Sciences at the University of Delaware. He received a Ph.D. in Computer Science at the University of Texas at Dallas in 2018. He received his BS degree in Mathematics and Applied Mathematics from Beijing Institute of Technology in July 2013. His research interests include computational social systems, machine learning, and theoretical computer science.

Zheng Dong is an assistant professor in the Department of Computer Science at Wayne State University. He received the PhD degree from the Department of Computer Science at the University of Texas at Dallas in 2019. His research interests include real-time cyber physical systems and mobile edge computing. He received the Outstanding Paper Award at the 38th IEEE RTSS. He is a member of the IEEE.

Cong Liu received the Ph.D. degree in computer science from the University of North Carolina at Chapel Hill, in Jul. 2013. He is an associate professor in the Department of Computer Science, University of Texas at Dallas. His research interests include real-time systems and GPGPU. He has published more than 30 papers in premier conferences and journals. He received the Best Paper Award at the 30th IEEE RTSS and the 17th RTCSA. He is a member of the IEEE.